

## Characterization and hydrogen generation of Zn-containing fullerene

Won Chun Oh<sup>a,\*</sup>, Ah-Reum Jung<sup>a</sup> and Weon-Bae Ko<sup>b</sup>

<sup>a</sup>Department of Advanced Materials & Science Engineering, Hanseo University, Chungnam 356-706, Korea

<sup>b</sup>Department of Chemistry, Sahmyook University, Seoul 139-742, Korea

In this study, the structural variations, surface states and mass transformation of fullerene [C<sub>60</sub>] derivatives are investigated through the preparation of an oxidized fullerene [C<sub>60</sub>O] and a Zn-containing fullerene compared to pristine fullerene [C<sub>60</sub>]. These were synthesized by an improved oxidation method using 3-chloroperbenzoic acid. From the XRD data, weak peaks of metallic zinc with pristine fullerene [C<sub>60</sub>] peaks were observed in the X-ray diffraction patterns for the Zn-containing fullerene. SEM micrographs for the metallic Zn-containing fullerene indicated that practically all the zinc introduced was located onto the carbon cages and consequently, it was dispersed into very small crystallites with growth of zinc metals. From the MALDI-TOF mass spectra, the differences in the spectra recorded on two types of fullerenes are due to the oxidation including chemical bonding and interposing of metallic zinc in the fullerene [C<sub>60</sub>] molecules. The FT-IR spectra gave additional information on the functional components on the surfaces of the Zn-containing fullerene. The EDX spectrum of Zn-containing fullerene showed the presence of C and O with strong Zn peaks. From the H<sub>2</sub> gas generation result, it is considered that a KOH concentration in the Zn-containing fullerene is a helpful factor in the hydrogen generation performance. A satisfactory hydrogen generation performance was achieved on a Zn-containing fullerene treated with an increase of KOH the concentration.

**Key words:** Fullerene [C<sub>60</sub>], XRD, SEM, EDX, MALDI-TOF mass spectra, Hydrogen generation.

### Introduction

Recently, the requirement for a safe, low cost and car-carry type hydrogen gas generator has become stronger because the use of fuel cells will be soon practical. However, problems are faced in the use of hydrogen as a transformation fuel as there is no suitable means of storage. Up to now a large number of fullerene complexes with different organic donors have been synthesized [1-3]. The complexes with fullerene are of a special interest as promising conducting materials and electric device materials [4, 5]. In the preparation of organometallic fullerene, C<sub>60</sub> itself served as a ligand with a transition metal [6]. This line of investigation has been intensely developed concerning the expansion of the circle of transition metals involved and also in the sense of using higher fullerenes. Synthesis of the molecules having both fullerene and metal fragments is of current interest because of the possible chemical coordination interactions between these groups. Fullerenes are known to be strong electron acceptors, whereas transition metallic groups may behave very different by due to the variety of metals and ligands. The degree of hydrogen generation between the donating and accepting parts of the same molecule should depend strongly on

the nature of a spacer. For the preparation of metallofullerenes, fullerene oxides and their isomers have been obtained by semiempirical studies in some research groups [7, 8]. The metallofullerenes remain exciting molecules combining the carbon cluster of simple fullerenes with the enhanced functionality of the treated metal species. The high solution electron affinities of the fullerenes along with the ionization potentials of the transition metals would result in an electron from the transition metal residing on the carbon cage and activated carbon [9]. Currently, carbon materials have been widely investigated for hydrogen storage, and very attractive results are reported for various carbon nanotubes [10], and activated carbons [11]. An important condition for the wide usage of hydrogen as a future fuel, especially for electrical vehicles, is the development of a safe, cheap and simple storage method. In the past years different storage technologies have been investigated [12, 13] to develop a secure and cheap way to store hydrogen. In this study, we will discuss our experimental results with the preparation of metallofullerene and their hydrogen generation. These types of material are expected to show promising applications in diverse areas, such as an electronic device material, as substrate materials for hydrogen generation and in the biological sciences.

In this study, we present the characterization and hydrogen production of some Zn-containing fullerenes. They were synthesized by an improved oxidation method. The structural variations, surface states and mass transformation of fullerene [C<sub>60</sub>] are investigated through the

\*Corresponding author:  
Tel : +82-41-660-1337  
Fax: +82-41-688-3352  
E-mail: wc\_oh@hanseo.ac.kr

preparation of an oxidized fullerene [ $C_{60}O$ ] and fullerenes [ $C_{60}$ ] treated with zinc sequentially after oxidation compared to pristine fullerene [ $C_{60}$ ]. X-ray diffraction (XRD), scanning electron microscopy (SEM), matrix-assisted laser desorption ionization time-of-flight (MALDI-TOF) mass spectrometry, energy dispersive X-ray (EDX) and FT-IR were conducted on these new species. Finally, we attempted an evaluation for Zn-containing fullerenes are presented in terms of results for the generation efficiencies of hydrogen.

## Experimental

### Materials

Pristine crystalline fullerene [ $C_{60}$ ] powder of 99.9% purity from TCI (Tokyo Kasei Kogyo Co. Ltd., Japan) was used as a starting material. Reagents for the treatment were purchased as reagent-grade from Duksan chemical Co and Daejung chemical Co. and used without further purification unless otherwise stated. All solvents were purified using standard procedures. Evaporation and concentration in a vacuum were done at water aspirator pressure and compounds were dried at 1.33 Pa.

### Chemical oxidation of fullerene and zinc treatments

*m*-chloroperbenzoic acid (MCPBA, ca. 0.96 g) was suspended in 60 ml benzene, and fullerene [ $C_{60}$ ] (ca. 40 mg) was added, the mixture was refluxed at air atmosphere for 6 h. And the solvent dried at the boiling point (353.13 K) of benzene. The solid precipitates were transformed to a dark brown color. After completion, these dark brown precipitates were washed with ethyl alcohol and then dried at 363 K. We prepared 0.1 M  $ZnCl_2$ , for the zinc treatment. Doubly distilled water was used to dissolve the chemicals to be free from impurities. For the treatment, 20 mg of oxidized fullerene [ $C_{60}O$ ] was dipped into 20 ml of a zinc ion dissolved aqueous solution and stirred for 6 h at room temperature. Finally, these samples were dried at 368 K for 72 hours in an air atmosphere.

### Instrumental analysis and characterization

X-ray diffraction patterns for the measurement of structural variations were taken using an X-ray generator (Shimatz XD-D1, Japan) with  $Cu K\alpha$  radiation. Scanning electron microscopy (SEM, JSM-5200 JOEL, Japan) was used to observe the surface states and structure of the oxidized fullerene [ $C_{60}O$ ] and Zn-containing fullerenes compared to pristine fullerene [ $C_{60}$ ]. For the elemental analysis in the pristine fullerene [ $C_{60}$ ], oxidized fullerene [ $C_{60}O$ ] and Zn-containing fullerenes, energy dispersive X-ray analysis (EDX) was also used. As one of the analytical procedures for the mass transformation for these samples, MALDI-TOF mass spectrometry (Voyager, DE-STR, U.S.A.) was used to characterize the structural transformation by oxidation and the behavior of Zn-treated fullerene. The two types of fullerene derivative were examined by a cyano-4-hydroxyl sinamic acid as the matrix using the spectroscopy. Reflectance mode FT-IR (Nicolet

380, U.S.A.) spectra were collected from the two types of fullerene samples with a smart miracle ATR method.

### $H_2$ gas collection

A schematic of the apparatus for  $H_2$  gas collection is shown in Fig. 1. Column (6) (the KOH supply tube) was always filled with KOH solution. After the sample reservoir was completely removed from the KOH solution, it was filled with Zn-containing fullerene. In this state, if the double cock (7) was opened, samples could be submerged in the KOH solution. Hydrogen gas generated in the sample reservoir was collected in the volumetric gauge (9).

## Results and discussion

Shown in Fig. 2 are the X-ray diffraction patterns of (a) oxidized fullerene [ $C_{60}O$ ] and (b) Zn-containing fullerene. XRD is a very important experimental technique that has long been used to address all issues related to the crystal structure of solids, including lattice constants and geometry, identification of unknown materials orientation of single crystals, preferred orientation of polycrystals, defects, stress, etc. From these results, it is seen that the Zn-containing fullerene in Fig. 2 (b) exhibits pristine fullerene peaks and some metallic peaks of weak intensity at around 11.5, 23, 25 and 60.5°. The peak positions from the oxidized fullerene [ $C_{60}O$ ], however, were not found to be different in position from the diffraction peaks from the pristine fullerene except a decrease in intensity. This is reasonable in that the attachment of O to graphene,

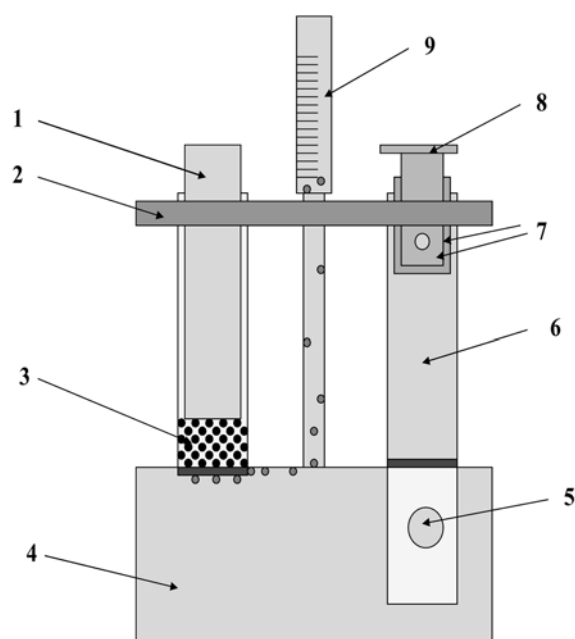


**Fig. 1.** Schematic apparatus for  $H_2$  gas collection from Zn-containing fullerene; 1. Syringe, 2. Supporter, 3. Sample, 4. KOH reservoir, 5. Hall, 6. KOH supply tube, 7. Double cock, 8. Rotational valve, 9. Volumetric gauge for  $H_2$  gas collection.

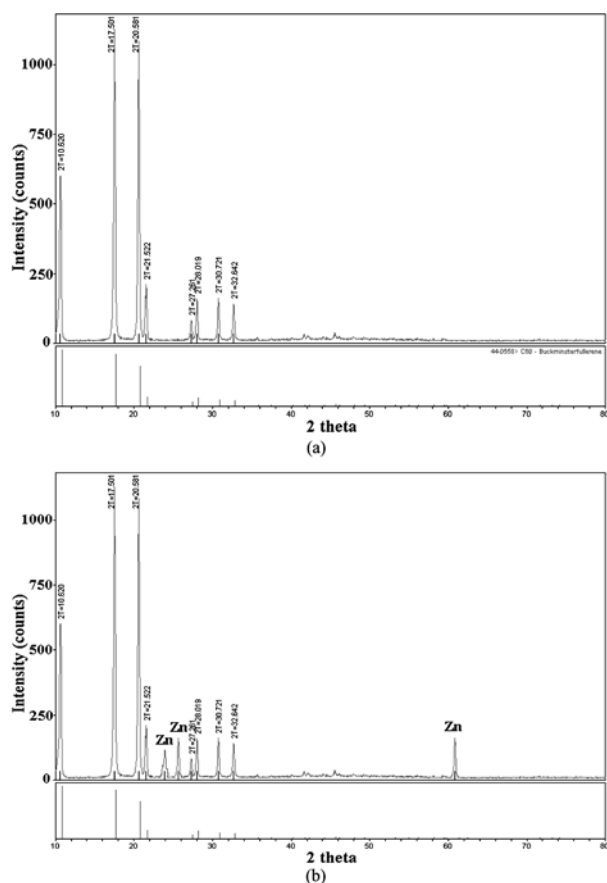


**Fig. 2.** XRD patterns of fullerene derivatives; (a) oxidized fullerene and (b) Zn-containing fullerene.

may be cause only a little change to the pristine structure of fullerene [ $C_{60}$ ] by the oxidation reaction. Therefore, it is concluded that the zinc treatment after oxidation yields a Zn-containing fullerene product with the XRD patterns distinguishable from that of pristine fullerene [ $C_{60}$ ], which may improve the amount of hydrogen production.

Figure 3 shows SEM micrographs of the fullerene [ $C_{60}$ ] sample series before and after oxidation, and after the zinc treatment. SEM is one of the most widely used techniques for obtaining topographical information and chemical composition information near the surface. The fullerene samples of (a) and (b) the pristine fullerene [ $C_{60}$ ], (c) and (d) the oxidized fullerene [ $C_{60}O$ ], and (e) and (f) the Zn-containing fullerene were examined by the technique to determine the surface structure and the formation of the metallic state on the surface. From these results, the characterization of surface texture on the fullerene [ $C_{60}$ ] samples before and after oxidation and the zinc distributions on the surfaces after zinc treatment were determined. SEM micrographs of the pristine fullerene [ $C_{60}$ ] sample provide information about the surface state of smooth surface and pebble-like  $C_{60}$ . After the oxidation treatment, it was shown that the surface properties were modified in some cases, this effect being a change to the surface state from the smooth pebble-like appearance of the pristine to a

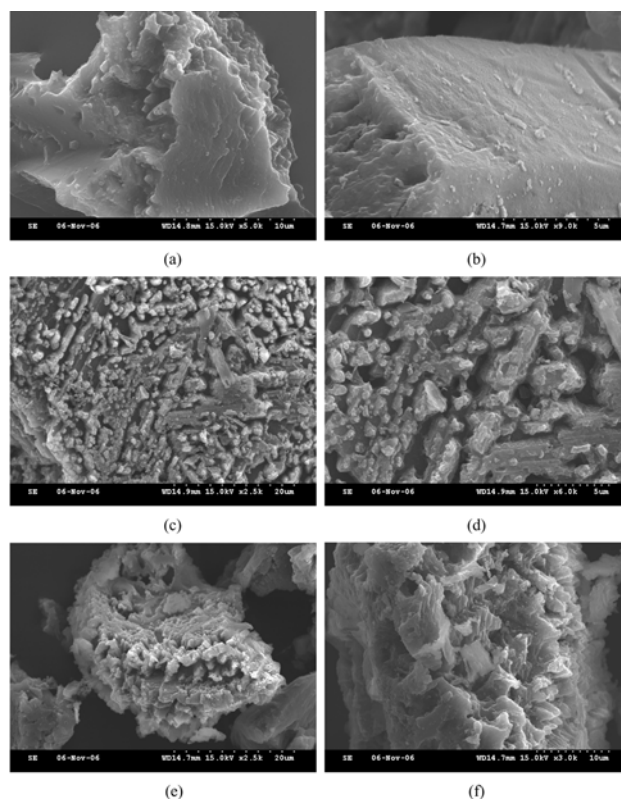


**Fig. 3.** SEM micrographs of pristine fullerene and fullerene derivatives; (a) and (b): pristine fullerene, (c) and (d): oxidized fullerene, and (e) and (f): Zn-containing fullerene.

coarse bread-like in the oxidized fullerene [ $C_{60}O$ ]. In case of Zn-containing fullerene, these observations indicated that the metallic zinc introduced is located on the external and internal surfaces of the carbon cages and inside fullerene pores and consequently, it is dispersed into very small particles of zinc crystallites. From these morphological changes, large Zn particles on the fullerene [ $C_{60}$ ] outer surfaces are clearly visible and resulted in the clogging and frost-like formation, as shown in Fig. 3(e) and (f). Finally, it is seen that the metallic Zn dispersed in and on the outside surfaces of fullerene [ $C_{60}$ ] is formed to give crystallites and aggregates.

To obtain further information, the structure of these prepared materials was studied by a combination of XRD analysis and MALDI-TOF mass spectroscopical measurements. The results of these measurements gave additional evidence of the difference of the two types of material. Details of the results obtained are in the MALDI-TOF mass spectra observed for the Zn-containing fullerene, as compared to the material transformed by oxidation. The preparation of fullerene oxides would be of great significance in the development of this newly cultivated field of chemistry. The traditional mass spectrum of pure fullerene [ $C_{60}$ ] has been shown in previous studies [14, 15]. The mass spectrum of fullerene [ $C_{60}$ ] transformed by oxidation is presented in Fig. 4(a). It shows major peaks for pristine fullerene [ $C_{60}$ ] at 720 m/z and oxidized fullerene [ $C_{60}O$ ] at 736.92 m/z.

Within the limits of the resolution this is consistent with the elemental composition  $C_{60}O$ . The MALDI-TOF mass analysis provides very clear evidence of a stable fullerene oxide formation with the  $C_{60}O$  structure. In Fig. 4 (a), it is confirmed that the O signals from oxidized fullerene [ $C_{60}O$ ] are at 752.68, 768.87, 784.85, 801.80 and 816.16 m/z. These results indicate that these dominant peaks of the spectrum correspond to increasing O in pristine fullerene [ $C_{60}$ ] by a structural transformation. MALDI-TOF mass spectrum of the Zn-containing fullerene is shown Fig. 4(b). The observation of a peak due to a trace of zinc appeared at 801.3 m/z. This is also consistent with the elemental composition  $C_{60}O \cdot Zn$ . The zinc has a strong tendency to oxidize and form stable compounds, which as a surface layer presents a direct interaction between the fullerene [ $C_{60}$ ] and metallic zinc. Taking this into account the differences in the spectra recorded on the two types of fullerene are due to the oxidation including chemical bonding and interposing of metallic zinc in the fullerene [ $C_{60}$ ] molecules. The differences in the spectra recorded on the two types of fullerene illustrate the influence by transformation of the chemical components (O and Zn) on the oxidation and zinc treatment process. This influence has its origin in the different chemical reactivity with

the fullerene [ $C_{60}$ ] substrate. The pristine fullerene [ $C_{60}$ ], however, may be not reacted with metallic elements without an oxidation process [16, 17].

For identification of the functional components on the surfaces, we observed that the FT-IR spectra could give additional information on quinone and benzene ring deformation on the surface of the Zn-containing fullerene. The FT-IR spectra for the fullerene derivatives are shown in Fig. 5. From the appearance of the absorption bands the differences between the oxidized fullerene [ $C_{60}O$ ] and Zn-containing fullerene are mainly seen to be due to the functional group deformations. As shown in Fig. 5(a) and (b), the  $\nu$  (C-O) mode of the methoxy groups depends on the chemical structure of the adsorption sites. Absorption of C-O followed by taking an IR spectrum has been used to characterize treated and non-treated metal-carbon composite catalysts [18]. The most characteristic changes are observed at  $1379.6\text{ cm}^{-1}$  in the presence of C-O- containing structures. The C-O- containing structures from an oxidation treatment are consequently associated with the homogeneous distribution of metallic zinc with an increased surface acidity of fullerene [ $C_{60}$ ]. The frequency of  $\nu$  (C-O) of adsorbed carbon monoxide is often treated as an indicator characterizing the local coordination. This is also suitable for examining the state of metal ions situated

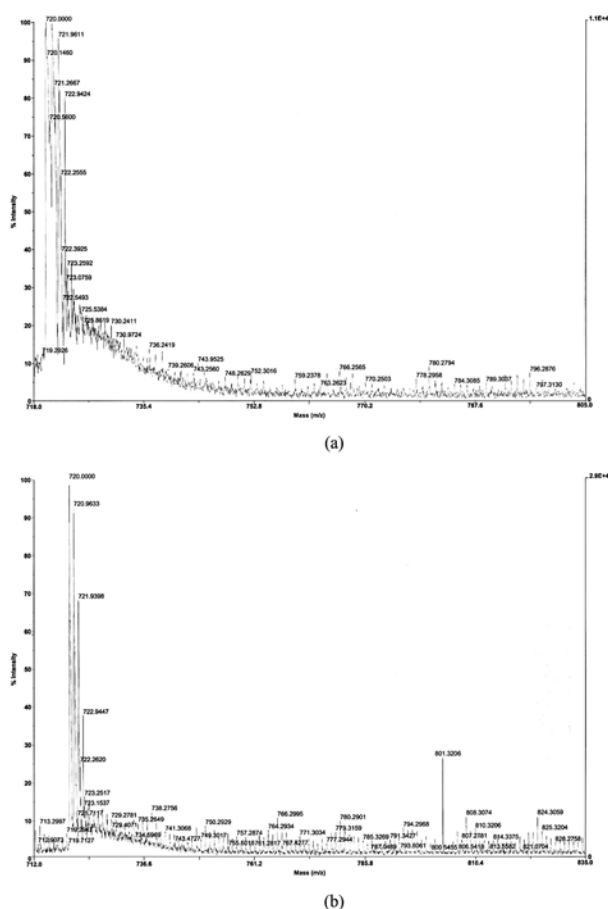


**Fig. 4.** MALDI-TOF mass spectra of fullerene derivatives; (a) oxidized fullerene and (b) Zn-containing fullerene.

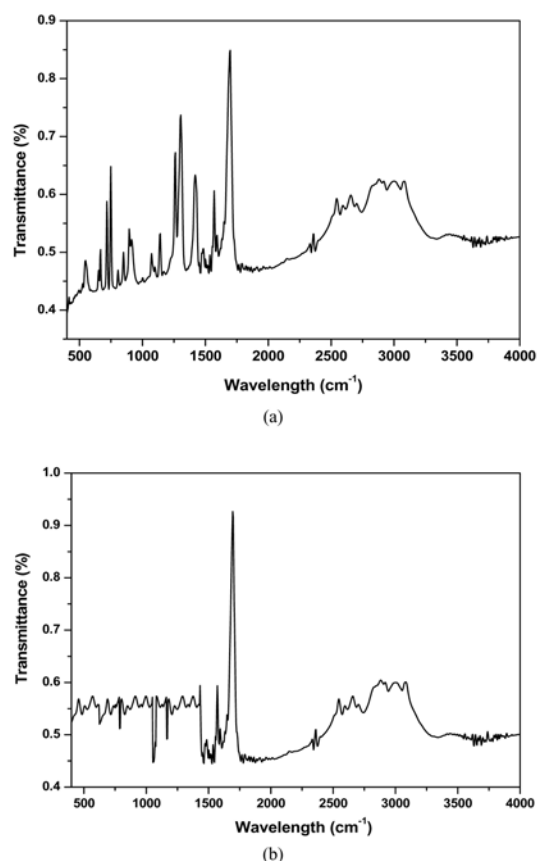


**Fig. 5.** FT-IR spectra of fullerene derivatives; (a) oxidized fullerene and (b) Zn-containing fullerene.

differently on the solid surface. The  $1165\text{ cm}^{-1}$  peak is assigned to a characteristic vibration mode quinone ring. The  $1530\text{ cm}^{-1}$  peak (stretching of quinoid rings) shows a red shift to  $1580\text{ cm}^{-1}$ , whereas the position of the benzenoid ring absorption at  $1500\text{ cm}^{-1}$  stays about the same. The weak band observed at  $2362.6\text{ cm}^{-1}$  is usually ascribed to the presence of aliphatic compounds. A broad band in the  $3100\text{--}3500\text{ cm}^{-1}$  region, typically attributed to O-H stretches from hydroxyl, phenolic and carboxylic groups, is absent. Thus FT-IR spectra confirm the formation of carbonyl groups during the oxidation process. The main goal of oxidation is to obtain a more hydrophilic surface with a relatively large number of oxygen-containing oxygen groups on the fullerene  $[\text{C}_{60}]$  surfaces.

For the elemental microanalysis of the Zn-containing fullerene, the sample was analyzed by EDX. This EDX spectrum of the Zn-containing fullerene is shown in Fig. 6. This spectrum shows the presence of C and O with strong Zn peaks. The spectrum was richer in C, O and major zinc metal than any other elements. The results of EDX elemental microanalysis of zinc-containing fullerene are listed in Table 1.

Most papers reporting about theoretical studies on the hydrogen absorption in carbon nanostructures focus on the physisorption of  $\text{H}_2$  on carbon at low temperature and high pressure [10, 19, 20]. Experiments on the hydrogen generation in carbon have been carried out

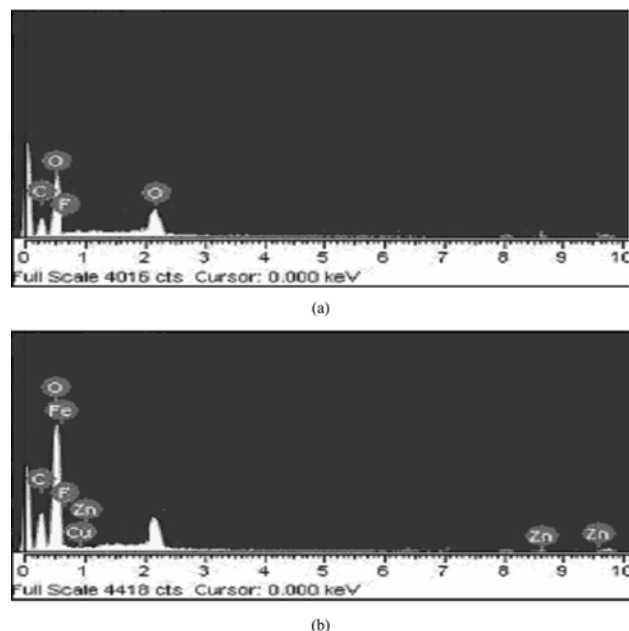


**Fig. 6.** EDX elemental microanalysis of fullerene  $[\text{C}_{60}]$  treated with zinc sequentially after oxidation; (a) oxidized fullerene and (b) Zn-containing fullerene.

**Table 1.** EDX Elemental Microanalysis of Prepared Zn-Containing Fullerene

Sample (wt.%)	C	O	Zn	Others
Oxidized Fullerene	55.6	42.5	0.12	1.81
Zn-Containing Fullerene	56.5	38.4	4.52	0.57

using different methods under various conditions and on many small and often not very well characterized samples. The hydrogen generation performance of the Zn-containing fullerene was investigated by treatment with various concentrations of KOH and the results are shown in Fig. 7. From these results, it is considered that a concentration of KOH with the Zn-containing fullerene is a helpful factor in the hydrogen generation performance. A satisfactory hydrogen generation performance was achieved on the Zn-containing fullerene treated with an increase of the KOH concentration. The amount of hydrogen generation was approximately proportional to the concentration of the alkali hydroxide (KOH). If a large amount of metal was incorporated on a carbon, the large amount of hydrogen gas can be obtained from a Zn-containing fullerene. Novel carbon materials, such as carbon nanotubes, activated carbons and carbon nanofibers have attracted much interest, however, the values for their hydrogen storage capacity scatter over several orders of magnitude [19]. At present, the independently confirmed and repeatable storage capacities in carbon materials at room temperature are less than 1 wt% [19, 21], however, higher values can be reached by lowering the temperature. The generation capacity is correlated to the physical parameters of the carbon samples. However, the generation stability and safety have to be considered as key factors for applications.

## Conclusions

The structural and morphological variations, and mass transformation of fullerene derivatives were inves-

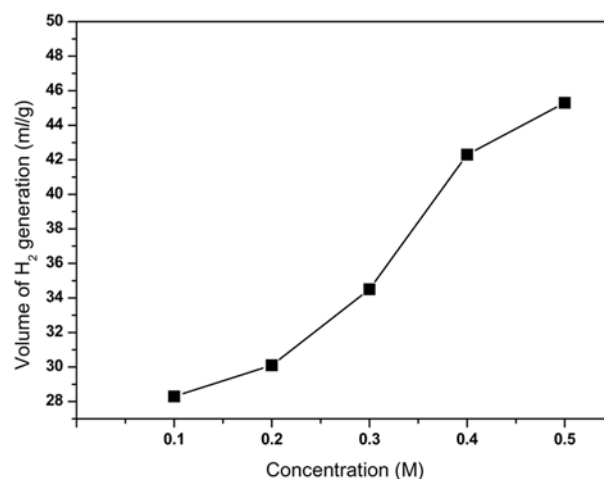


**Fig. 7.** Hydrogen generation capacities of a Zn-containing fullerene with a variation of KOH concentration.

tigated through the preparation of an oxidized fullerene [C<sub>60</sub>O] and Zn-containing fullerenes and compared to a pristine fullerene [C<sub>60</sub>]. XRD, SEM, MALDI-TOF mass spectrometry, FT-IR and EDX analysis were conducted for these samples to obtain new information. From the XRD data, new peaks of zinc with pristine fullerene [C<sub>60</sub>] peaks were observed in the X-ray diffraction patterns for the Zn-containing fullerene. SEM micrographs for the Zn-containing fullerene indicated that metallic zinc particles were dispersed as very small crystallites with growth of zinc particle and located inside and outside fullerene cages and pores. From the MALDI-TOF mass spectra, the differences in the spectra recorded on two types of fullerene are due to the oxidation including chemical bonding and the incorporation of metallic zinc in the fullerene molecules. The appearance of the absorption bands from the FT-IR spectra showed that the differences between the oxidized fullerene [C<sub>60</sub>O] and Zn-containing fullerene are mainly due to functional group deformations. Finally, the EDX spectrum of the Zn-containing fullerene showed the presence of C and O with strong Zn peaks. From the H<sub>2</sub> gas generation results, it is considered that a KOH concentration for the Zn-containing fullerene are a helpful factor to the hydrogen generation performance. Satisfactory hydrogen generation efficiency was achieved on a Zn-containing fullerene treated with increasing of KOH concentrations.

### References

1. J. Fink, T. Pichler, M. Knupfer, M. S. Golden, S. Haffner, R. Friedlein, U. Kirbach, P. Kuran and L. Dunsch, *Carbon*, 36 (1998) 625-631.
2. B. Pietzak, M. Waiblinger, T. Almeida Murphy, A. Weidinger, M. Hohne and A. Hirsch, *Carbon*, 36 (1998) 613-615.
3. H. Shinohara, Endohedral metallofullerene, *Rep. Prog. Phys.*, 63 (2000) 843-92.
4. C.J. Nuttall, Y. Hayashi, K. Yamazaki, T. Mitani and Y. Iwasa, *Adv. Mat.*, 14 (2002) 293-296.
5. G. Cao, *Nanostructures and nanomaterials*, Imperial college press, p.230 (2004).
6. V.I. Sokolov, M.N. Nefedova, T.V. Potolokova and V.V. Bashilov, *Pure Appl.Chem.*, 73 (2001) 275-278.
7. B.C. Wang, L. Chen, K.J. Lee and C.Y. Cheng, *J. molecular structure*, 469 (1999) 127-134.
8. D. Heymann, S.M. Bachilo, B.B. Weisman, F. Cataldo, R.H. Fokkens, N.M.M. Nibbering, R.D. Vis and L.P.F. Chibank, *J. Am. Chem. Soc.*, 122 (2000) 11473-11479.
9. W.C. Oh, M.L. Chen and Y.S. Ko, *Carbon Science*, 8 (2007) 6-11.
10. C. Liu, Q.H. Yang, Y. Tong, H.T. Cong and H.M. Cheng, *Applied Physics Letters*, 80 (2002) 2389-91.
11. K. Jurewicz, E. Frackowiak and F. Beguin, *Fuel Processing Technology*, 77 (2002) 415-421.
12. A. Zuttel, *Mater Today*, 6 (2003) 24-33.
13. M. Hirscher and M. Becher, *J. Nanosci Nanotech*, 3 (2003) 2-17.
14. B. Burger, H. Kuzmany, T.M. Nguyen, H. Sitter, M. Walter, K. Martin and K. Kullen, *Carbon*, 36 (1998) 661-663.
15. Z. Gu, L. Zhang, J.L. Margrave, V.A. Daveydov, A.V. Rakhmanina, V. Agafonov and V.N. Khabashesku, *Carbon*, 43 (2005) 2989-3001.
16. W.C. Oh, A.R. Jung, W.B. Ko and C.H. Jung, *The proceeding of the 33<sup>rd</sup> annual meeting on carbon materials*, Carbon Society of Japan, pp 162-163, (2006).
17. M. Baibarac, L. Mihut, N. Preda, I. Baltog, J.Y. Mevellec and S. Lefrant, *Carbon*, 43 (2005) 1-9.
18. W.C. Oh, C.S. Park, J.S. Bae and Y.S. Ko, *Carbon Science*, 7 (2006) 34-41.
19. M. Ritschel, M. Uhlemann, O. Gutfleisch, A. Leonhardt and C. Taeschner, *Appl. Phys. Lett.*, 80 (2002) 2985-7.
20. B.T. Tarasov, Y.M. Shul'ga, O.O. Lobodyyuk and O.F. Onipko, *Proc. SPIE*, 4806, (2002) 197-206.
21. X. Chen, M. Haruska, M. Becher, U. Dettlaff-Weglis-kowka, M. Hirscher, M. Becher and S. Roth, *Mater. Res. Soc. Symp. Proc.*, 706, 9-11 1-6 (2002).